Hindawi
Science and Technology of Nuclear Installations
Volume 2018, Article ID 1896309, 16 pages
https://doi.org/10.1155/2018/1896309

Research Article

Preliminary Selection of Device Materials to Locally Transform Thermal into SFR Neutron Spectrum

N. Chrysanthopoulou,[1,2] P. Savva,[1] M. Varvayanni,[1] C. Colin,[3] C. Huot-Marchand,[3] and N. Catsaros[1]

[1]*National Centre for Scientific Research "Demokritos", Institute of Nuclear & Radiological Sciences & Technology, Energy & Safety, Greece*
[2]*National Technical University of Athens, School of Applied Mathematical and Physical Sciences, Department of Physics, 15780 Zografou, Greece*
[3]*CEA-DEN-DER, JHR Project, Cadarache, France*

Correspondence should be addressed to P. Savva; savvapan@ipta.demokritos.gr

Received 14 May 2018; Revised 25 July 2018; Accepted 31 July 2018; Published 2 September 2018

Academic Editor: Keith E. Holbert

The safe introduction of Generation IV (Gen IV) reactor concepts into operation will require extensive testing of their components. This must be performed under neutronic conditions representative of those expected to prevail inside the new reactor cores when in operation. In a thermal Material Testing Reactor (MTR) such neutronic conditions can be achieved by tailoring the prevailing neutron spectrum with the utilization of a device containing appropriate materials. In this work various materials are investigated as candidate components of a device that will be required in case that a thermal MTR neutron energy spectrum must be locally transformed, so as to imitate Sodium cooled Fast Reactor (SFR). Many nuclides have been examined with respect to only their neutronic behavior, providing thus a pool of neutronically appropriate materials for consideration in further investigation, such as regarding reactor safety and fabrication issues. The nuclides have been studied using the neutronics code TRIPOLI-4.8 while the reflector of the Jules Horowitz Reactor (JHR) was considered as the hosting environment of the transforming device. The results obtained suggest that elements with important inelastic neutron scattering could be chosen at a first level as being able to modify the prevailing neutron spectrum towards the desired direction. The factors which are important for an effective inelastic scatterer comprise density and inelastic microscopic cross section, as well as the energy ranges where inelastic scattering occurs. All the above factors have been separately examined in order to suggest potential device materials, able to locally produce SFR neutron spectrum imitation in a thermal MTR.

1. Introduction

Several advanced SFR concepts (such as ASTRID, JSFR, PRISM, PGSFR, BN-1200, and CFR-600) are under development in a new phase of fast reactors (FRs) design [1]. The concept of SFR has been selected by the Generation IV International Forum (GIF) as a promising nuclear energy system able to fulfill the Generation IV criteria: enhanced safety, economic competitiveness, reduction in environmental burden, and efficient utilization of resources as well as proliferation resistance and enhanced physical protection [2]. With the perspective to put into operation the above type of reactors, extensive research related to the behavior of the structural materials and the fuel under irradiation (during nominal and transient operation) is mandatory, comprising also relevant studies for the fuel fabrication and the pin cladding and wrapper material [3–6]. Thermal Material Testing Reactors (MTRs) are key facilities to perform experimental irradiation with the above-mentioned requirements [7] since Fast Experimental Reactors are very rare (only a few of them are in operation around the world).

Towards this aim several devices have been designed in thermal MTRs such as in BR2, HFR, ATR, MITR, HFIR, OSIRIS, BRR, Halden, and CABRI, in past years [8–16, 16–22, 22–37]. The most common approach to create fast irradiation conditions in a thermal MTR environment is by

implementing appropriate neutron absorbing "filters" (neutron screens or shields), reducing the thermal component of the neutron spectrum, such as boron, europium, cadmium, and hafnium [7]. These materials are characterized by high thermal neutron absorption cross sections and are almost transparent to fast neutrons. In principle the material selection depends on the specific reactor irradiation conditions and on the targeted neutron spectrum. It is also determined by factors such as the reactor safety, the reactor type in which the screening material will be inserted, the reactor coolant, and the available space for the neutron screen. Especially for the neutron screen selection, appropriate information must be available, since its behavior under irradiation conditions must be taken into account. Occasionally, the thermal neutron filters can be combined with a booster (fissile material) for further enhancing the fast neutron flux inside the facility (see, for example, [7, 20, 25]).

In this work an extensive computational study has been carried out for determining materials which, interacting with the neutron population distributed in the reflector area of the thermal JHR, can render the final local neutron distribution similar or as close as possible to that of SFR. The JHR reflector area was selected for the tests since one main objective of this reactor is to investigate and study structural materials for current and future generations of power plants; this task requires the development of appropriate devices. The output of the present work is a first pool of materials which could be possibly contained in a screening device for locally modifying the neutron spectrum. More specifically SFR spectrum simulation is attempted in an irradiation position of the JHR reflector. For this study the TRIPOLI-4.8 has been used.

It should be noted that the introduction of a neutron screen device in a reactor's irradiation facility demands the prior examination of the impact that it might have on the general reactor operation and safety. Before the actual insertion of the device in the reactor, an extensive work emphasizing reactor safety and performance aspects must be carried out. That is, the determination of the final device configuration is a multitask project comprising various analyses. The first step should be a study on the materials' effect on the neutron spectrum as far as their physical (e.g., density) and neutronic (i.e., microscopic cross sections for the various reactions) properties are concerned. The subsequent investigation steps before the neutron screen insertion should comprise various topics regarding at least (a) the device impact on the reactor reactivity and on the neighboring experiments, (b) the thermophysical properties of the screen, (c) the energy deposition on the screen material, (d) the ageing of the screen device under neutron irradiation, (e) the cooling of the screen, (f) the depletion rate of the screen material under irradiation, and (g) matters related to the device fabrication and postirradiation handling and treatment. The present study focuses only on the first step of a complete investigation towards the goal of achieving the desired neutron spectrum modification; that is, it deals with the neutronic behavior of each screening material. By examining a large range of different screening materials, the present analysis constitutes the basis for all the subsequent steps. Regarding in particular the cooling of the screen, the present work considers cooling materials which are found to have a negligible effect on the neutron spectrum.

2. The Jules Horowitz Material Test Reactor (JHR)

JHR [40] is a thermal MTR under construction at Cadarache Center in southern France and is intended to be the MTR which achieves the most important Research Reactor experimental capacity in Europe [41] within the next decade. This pool-type MTR is cooled by light water (two cooling systems) and is designed to have a maximum power of 100 MWth. The cylindrical core is of 71 cm diameter and 70 cm height, surrounded by a beryllium reflector of 35 cm thickness. The reactor has 37 positions for fuel rods location. The fuel rod is ring-shaped, with external and internal diameter of 9.5 cm and 3.7 cm, respectively, forming a central hole for irradiation purposes or control rod insertion; there are 27 fuel rods equipped to host control rods. The fuel rod is constituted of 3x8 convex, concentric plates of U_3Si_2 fuel, cladded with aluminum and cooled by light water circulating in water channels of 0.184 cm width. Schematic presentations for the JHR core and fuel rod are given in Figures 1 and 2. The design thermal flux is $5.2{\cdot}10^{14}$ n/cm^2/s and the fast flux (here E> 0.9MeV) is $5{\cdot}10^{14}$ n/cm^2/s [42]. The reactor will offer modern irradiation experimental capabilities for studying material and fuel behavior under irradiation. It will be a flexible experimental infrastructure to meet industrial and public needs related to Generation II, III, and IV Nuclear Power Plants (NPP) and to different reactors technologies [43]. JHR is designed to provide high neutron flux (higher than the maximum available today in most European MTRs), to perform instrumented experiments in order to support advanced modelling predictions beyond experimental points, and to operate experimental devices under various conditions (temperature, flux, coolant chemistry, stress, pressure, etc.) relevant to water reactors, gas cooled thermal or fast reactors, sodium fast reactors, etc. [42].

For this work a model of the reactor provided by TRIPOLI-4.8 [44] was utilized. The JHR core as simulated by TRIPOLI-4.8 is shown in Figure 3(a). A series of calculations concerning the introduction of a device in the reflector area of JHR was carried out. The available diameter in this area is 108mm. The device, each time constituted by different materials, was considered to be introduced in the location indicated in Figure 3(a), while Figure 3(b) gives the dimensions of the irradiation facility. The latter is assumed to be of a typical configuration (cylindrical, consisting of void). As can be seen a cylindrical irradiation space of 2.0 cm diameter is considered leaving thus a ring of sufficient thickness (i.e., 4.4 cm) to put the tested screening material, which should constitute a concentric ring placed in the available space.

3. Neutron Spectrum Characteristics of SFR

The use of sodium for cooling a FR provides a neutron energy spectrum in which the fission neutrons' flux maximum is shifted to lower energies comparing to other fast reactors spectra [45], while the neutron population distribution

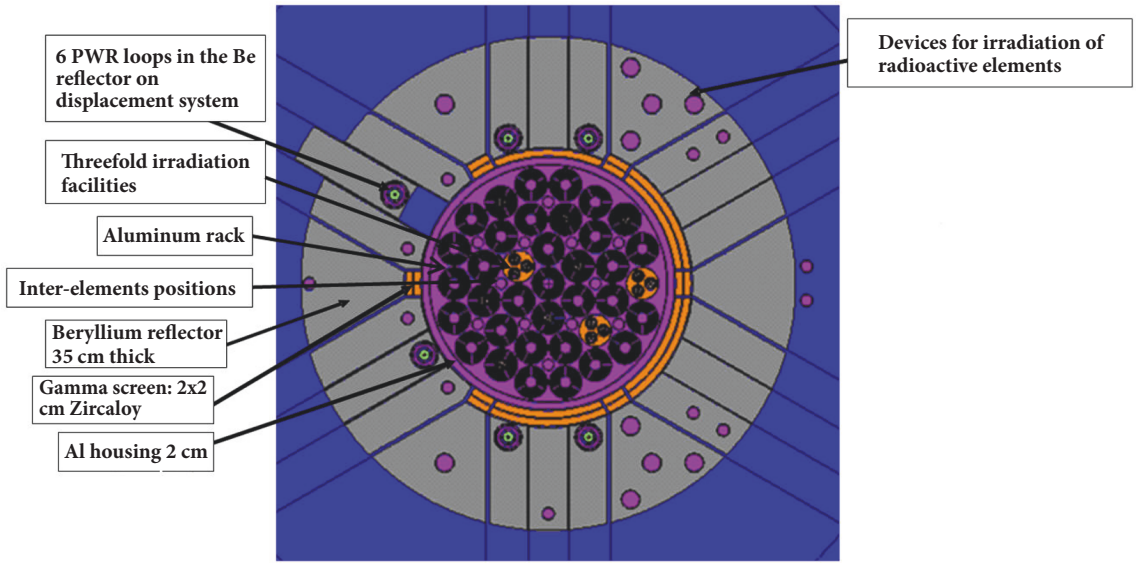

Figure 1: JHR cross section at the core middle plane. Cylindrical fuel assemblies (black) are located in an aluminum rack surrounded by an aluminum vessel (both purple); the Beryllium reflector (grey) allows locating many devices; some Zircaloy screens (orange) are also visible.

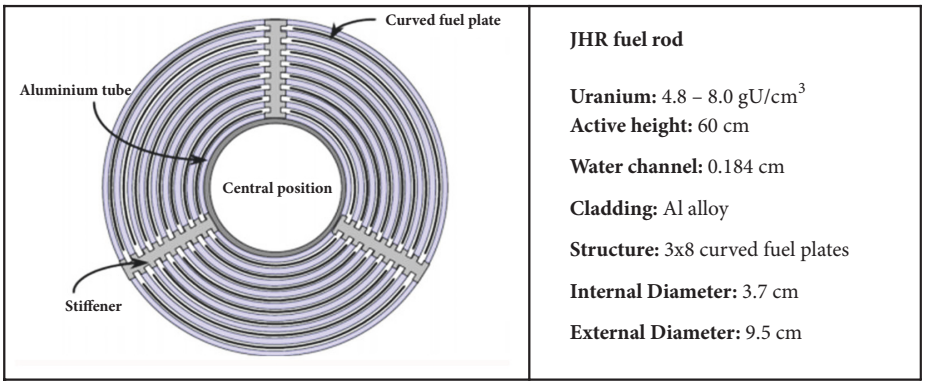

Figure 2: JHR fuel rod cross section.

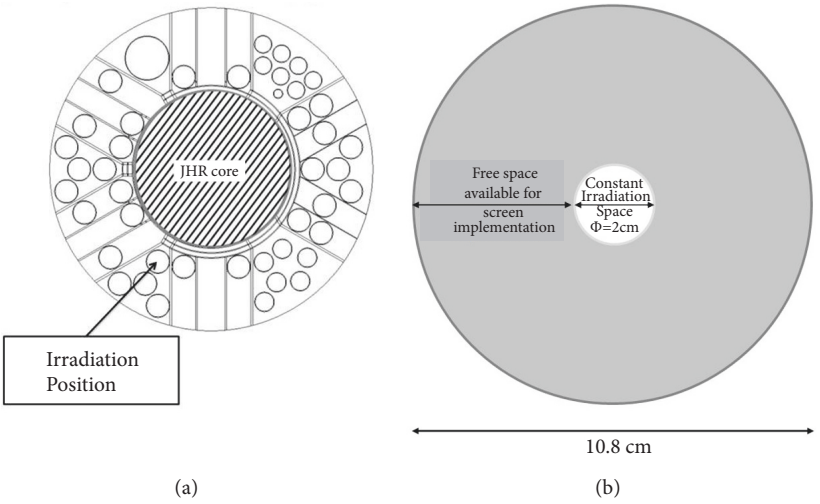

Figure 3: Horizontal cross section of (a) the JHR core as simulated by TRIPOLI-4.8. The arrow points towards the hosting irradiation facility in the reflector which was used for the calculations presented in this work. (b) The considered irradiation device. The available diameter of the JHR location indicated in (a) is 10.8 cm. The screening material is contained in the ring between 2.0 and 10.8 cm, leaving thus a sufficient amount of space for irradiation sample insertion.

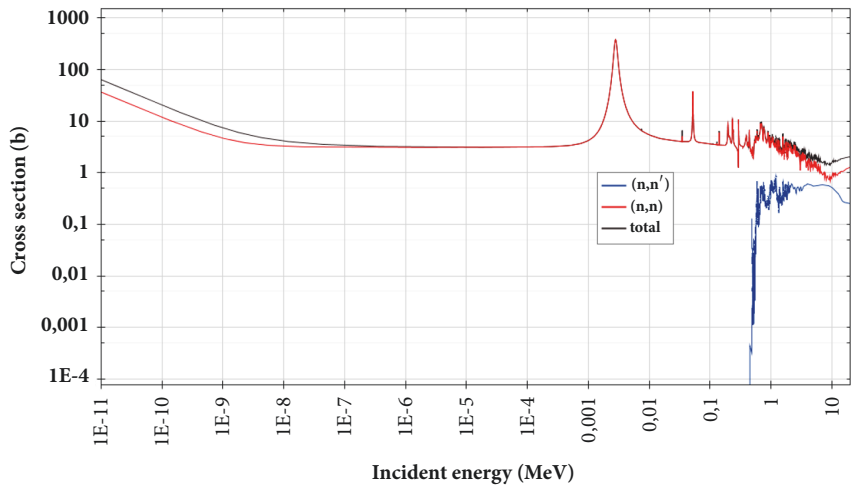

FIGURE 4: Total, elastic, and inelastic microscopic cross sections of ^{23}Na as produced by using the JEFF-3.1.1 Library [38] and the JANIS software [39].

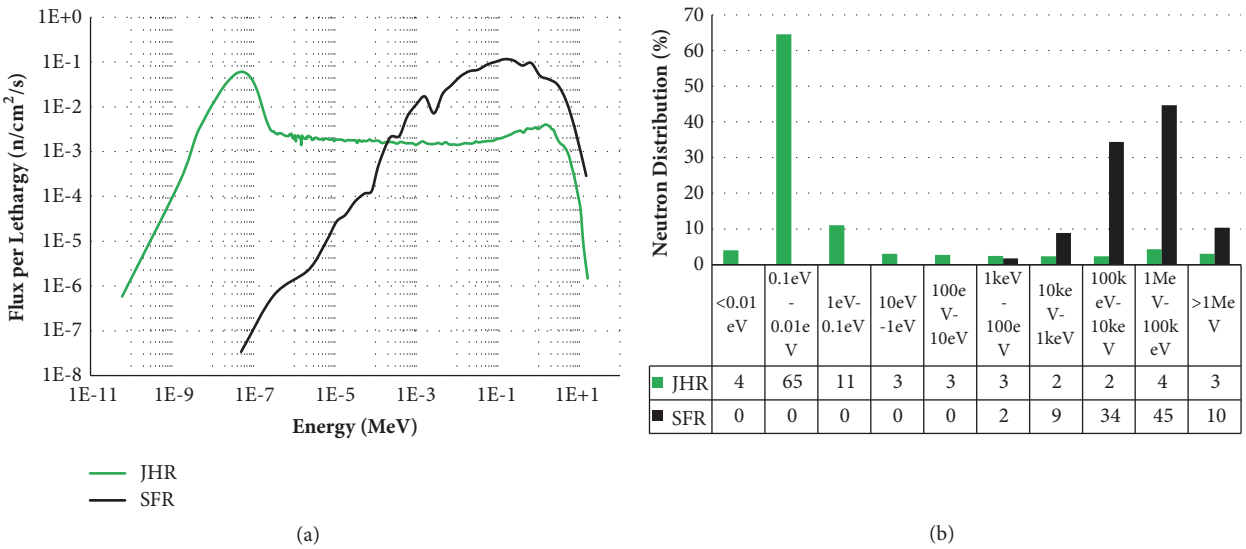

FIGURE 5: Comparison of the two reference spectra, assuming void in the irradiation facility; (a) neutron flux normalized to lethargy in JHR reflector (green line) and SFR (black line) and (b) neutron distribution per energy group (in %) for SFR (black) and JHR reflector (green).

around the maximum is broader (see Figure 5(a)). The softening of the spectrum is caused by both inelastic and elastic scattering of sodium. As stated in [46] sodium degrades the spectrum at high end as a result of inelastic scattering and builds up the low end of the spectrum by elastic scattering. The total, elastic, and inelastic microscopic cross sections of ^{23}Na are plotted in Figure 4, as produced by using the JEFF-3.1.1 Library [38] and the JANIS software [39]. In this work a reference SFR spectrum has been utilized, provided by the neutronic data of the prototype SFR reactor Phenix [47, 48]. Phenix was a 565 MWth SFR; description of the main Phenix characteristics can be found in [49].

4. Problem Outline

As already mentioned this work is a feasibility study for the identification of neutron screen materials which can locally modify a thermal neutron energy spectrum, so as to be as close as possible to that characterizing SFR. The neutron spectra of JHR reflector and SFR are illustrated in Figures 5(a) and 5(b). In Figure 5(b) the neutron distribution normalized to lethargy is partitioned in ten energy groups. The JHR reflector reference spectrum has a typical energy distribution of a thermal reactor, exhibiting two peaks. That is, the first peak occurs at low energies (below 0.1eV) due to the neutron thermalization (water- and reflector-induced) and the second at high energies (~1MeV) corresponding to the neutrons produced by fission. On the contrary, the thermal range of the SFR spectrum includes an insignificant number of neutrons, the latter being concentrated at energies of order of magnitude between 10^3 and 10^6 eV. Prompt neutrons are born at energy ranges from 0.1 to 10 MeV but the fast neutron spectrum component is shifted to lower energies due to the elastic and inelastic scattering interactions of fast neutrons

Table 1: Elements with the highest absorption capability classified with descending thermal microscopic absorption cross sections (σ_α).

Element	Symbol	Atomic number	σ_α (barns)	Reasons to reject
Gadolinium	Gd	64	49000	-
Samarium	Sm	62	5922	-
Fermium	Fm	100	5800	Large Z
Europium	Eu	63	4600	-
Californium	Cf	98	2900	Large Z
Cadmium	Cd	48	2450	-
Plutonium	Pu	94	1017.3	Large Z
Dysprosium	Dy	66	920	-
Boron	B	5	767	-
Berkelium	Bk	97	710	Large Z
Actinium	Ac	89	515	Large Z
Iridium	Ir	77	425	-
Mercury	Hg	80	374	Problematic properties[1]
Protactinium	Pa	91	200.6	Large Z
Neptunium	Np	93	180	Large Z
Promethium	Pm	61	168.4	Rare
Einsteinium	Es	99	160	Large Z
Erbium	Er	68	160	-
Rhodium	Rh	45	144.8	Rare
Hafnium	Hf	72	104	-

[1] High toxicity, high vapor pressure even at room temperature, low boiling point, producing noxious fumes when heated, and relatively low thermal conductivity.

with sodium as well as structural and other materials existing in SFR. This study intends to suggest materials which can affect the JHR spectrum in order for the two curves of Figure 5 to coincide as much as possible; these materials could then be indicated for further tests in the prospect to determine the appropriate device.

The methods of spectrum tailoring can only rely on the utilization of neutron interactions. To achieve the targeted neutron spectrum tailoring inside a thermal MTR, two options exist, i.e., either to remove the thermal spectrum component or to increase the fast/thermal neutrons ratio, using the appropriate neutron screens. This appropriateness is related to the screening materials' macroscopic cross sections (combining both physical and neutronic properties) of the various interactions they are involved in. In the following chapter the effect of different neutron interactions will be examined in view of achieving the desired result.

5. Simulation Procedure

The JHR reactor was here simulated with TRIPOLI-4 code, version 8.1 [44]. TRIPOLI-4 is dedicated to nuclear reactor physics and nuclear processes simulation. The code is composed of six software libraries: a geometry library, a cross section reading library derived from NJOY [50] I/O Fortran routines, a memory management library, a simulation library, and two special libraries enabling parallel calculations [51]. TRIPOLI-4 is used essentially for four major classes of applications: shielding studies, criticality studies, core physics studies, and instrumentation studies. The neutron energy domain of TRIPOLI-4 ranges from 10^{-5} eV to 20MeV, while, for photons, electrons, and positrons it ranges from 1 keV to 20 MeV [52]. The cross sections used by the code can be either continuous (pointwise) in ENDF-format or multigroup calculated by the APOLLO2 code [53]. Any pointwise cross section data in ENDF-6 format may be used, i.e., JEFF2, ENDF/B-VI, JEFF3, ENDF/B-VII, and JENDL4.3 [52]. For the present work the pointwise cross sections from the JEFF-3.1.1 [54] have been used.

Using TRIPOLI-4 the effect of different neutron interactions is separately examined in the following sections. As mentioned above the screening material is considered to constitute a concentric ring with the irradiation space, with a thickness that allows positioning in the 4.4 cm space shown in Figure 3(b). The presented neutron distributions have been calculated in the central irradiation space.

5.1. Effect of Materials with Important Absorbing or Fissioning Capability. The hardening of the thermal neutron spectrum can be achieved either by the utilization of thermal absorbers or by the introduction of fission sources (boosters), enhancing thus the fast component of the neutron spectrum (Chrysanthopoulou et al., 2014a). In a preliminary work [55] an extensive study was carried out using screening materials that have important absorbing capacity of thermal neutrons. This work was continued in more depth in [56]. The results obtained by the above analysis are here briefly outlined.

In Table 1, twenty of the stronger absorbing chemical elements, as found in the literature [57], are listed. The neutron capture cross section and the atomic number of each isotope are also reported. The last column contains brief comments about materials which are possibly unsuitable for use:

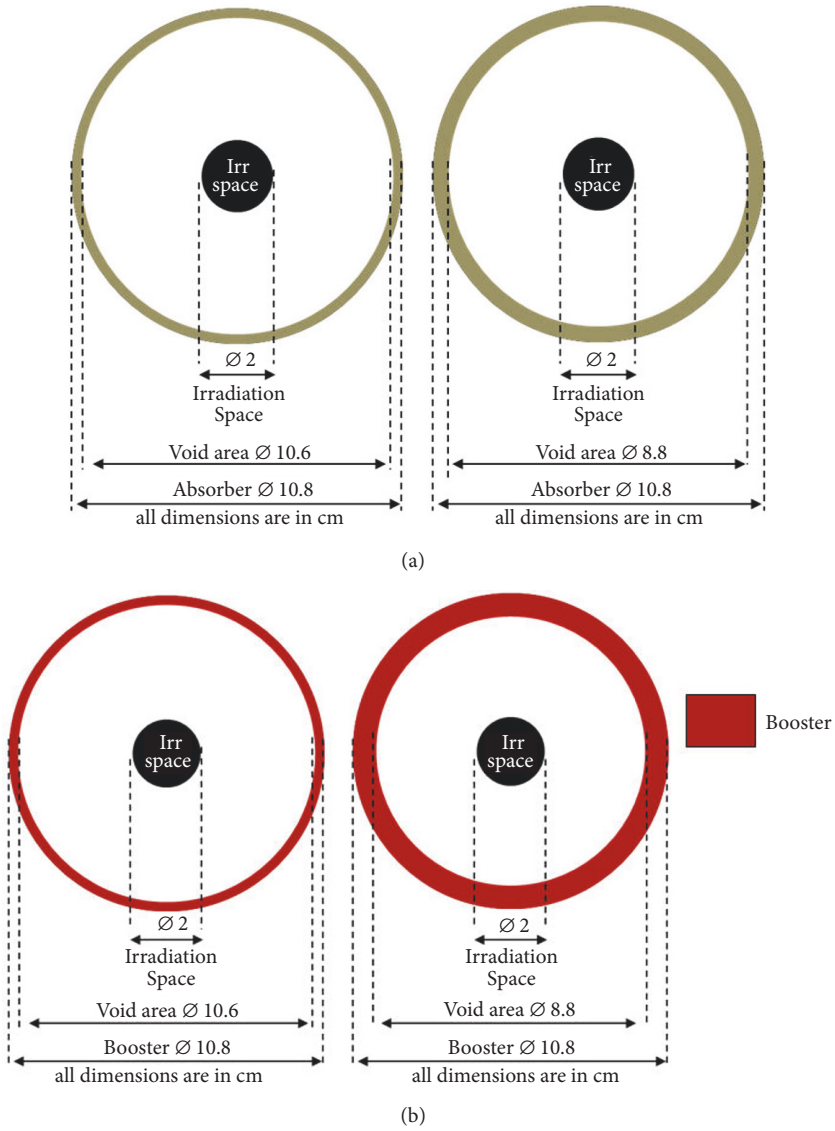

Figure 6: Irradiation device of two different thicknesses constituted by (a) absorbing material and (b) fissile material.

(a) Actinides such as Fm, Cf, Pu, Bk, Ac, Pa, Np, and Es are all fissionable nuclides and thus should not be considered as candidate absorbing materials. (b) Pr and Rh are rare elements and thus are not taken into account. (c) The physical properties of Hg do not allow its usage inside the reactor. The remaining nine elements, i.e., Sm, Gd, Eu, Cd, Dy, B, Ir, Er, and Hf, are not prohibitive for use inside a reactor's environment and thus were further investigated.

Assuming two "marginal" thicknesses of the tested material (i.e., 0.1 cm vs 1.0 cm) (Figure 6(a)), the effect on the reference neutron spectrum (i.e., in the JHR reflector) was examined.

Furthermore, in order to improve the obtained result, a neutron screen composed of fissile material (uranium 20% enriched in ^{235}U) was also investigated by successively increasing the screen thickness (Figure 6(b)).

All the examined nonfissile materials, even when considered of 0.1 cm thickness, were found to be able to provide a strong reduction of the reference thermal neutron component. As expected, the utilization of fissile material enhanced the fast spectrum component while at the same time the peak of the fast neutrons flux was shifted to lower energies. However, despite all these effects, the above study showed that the neutron screens when based only on neutron absorbing reactions or even on boosters are rather insufficient to successfully simulate the SFR spectrum. A centralized result is shown in Figures 7 and 8, for nonfissile and for fissile materials, respectively, the former of 1.0 cm and the latter of variable thickness of screening material. It should be noted that the metallurgy of the booster (i.e., constructive components) is not taken into account here since only the fissile material is examined as possible spectrum modifier.

5.2. Effect of Materials with Important Elastic Scattering Capacity. The findings of the above section stressed the

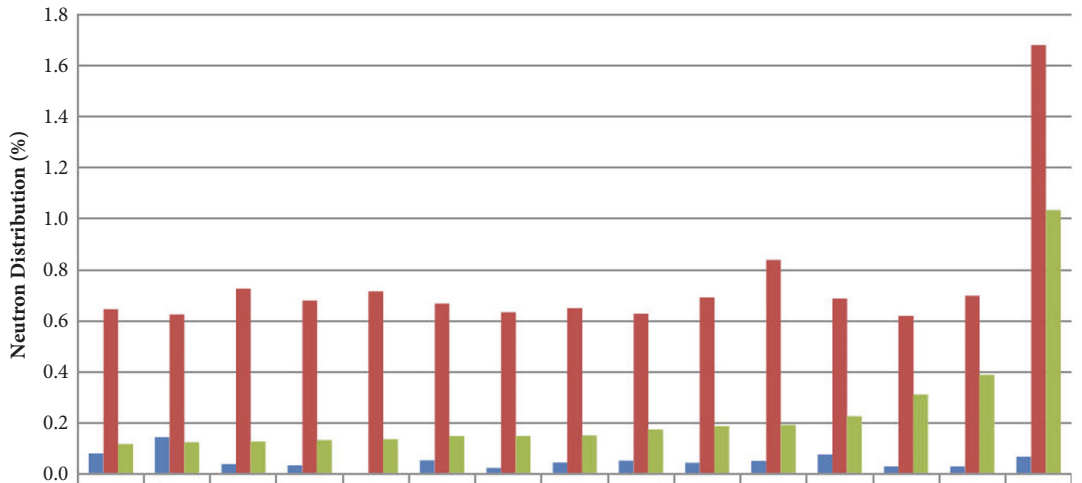

	ER167	DY	IR	IR191	CD113	HF177	GD157	DY164	EU	EU151	B10	GD155	DY161	GD	HF
< 0.01 eV	0.1	0.1	0.0	0.0	0.0	0.1	0.0	0.0	0.1	0.0	0.1	0.1	0.0	0.0	0.1
0.01 - 0.1 eV	0.6	0.6	0.7	0.7	0.7	0.7	0.6	0.7	0.6	0.7	0.8	0.7	0.6	0.7	1.7
0.1 -1 eV	0.1	0.1	0.1	0.1	0.1	0.1	0.2	0.2	0.2	0.2	0.2	0.2	0.3	0.4	1.0

Figure 7: Neutron population distribution at three thermal energy groups (1-0.1eV, 0.1-0.01eV, and <0.01eV) for all tested materials at 1.0 cm thickness.

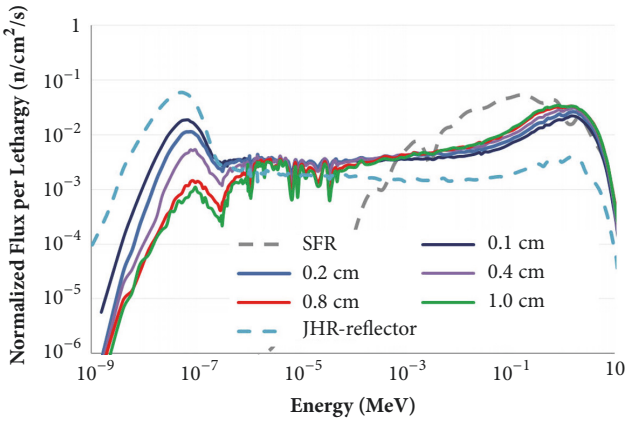

Figure 8: Effect of different thicknesses of booster (0.1, 0.2, 0.4, 0.8, and 1.0 cm) on the neutron spectrum. SFR and JHR reflector neutron spectra are also depicted.

requirement of investigating the effect of the neutron scattering interactions.

Elastic scattering is significant all over the neutron energy range of a thermal reactor (1·10-11 to 20 MeV). In the present subsection the possibility of achieving the SFR spectrum imitation through elastic neutron scattering on the screening material is investigated. The study was based on the consideration that the elements that present important elastic cross section at the energies around 1 MeV could be utilized to achieve the desired result. Moreover, seeing that the higher the material density the more favoured the scattering interaction, only solid materials were searched. The gaseous elements were excluded from this analysis since their low density would make them transparent to neutrons. After

Table 2: Selected isotopes and their densities.

Element	Density (g/cm^3)
^{36}S	1.96
^{39}K	0.86
^{40}K	0.86
^{48}Ca	1.55
^{138}Ba	3.51
^{139}La	6.15
^{197}Au	19.30

an extensive analysis throughout the periodic table, using also ENDF library and JANIS software, it was found that only a few isotopes exhibit an intense peak of scattering cross section at the desired energy range (Table 2). In all cases this peak is observed above 2MeV and mainly around 3MeV. At this point it should be stressed that the above elements present also important inelastic cross section. Although a possible requirement of isotope separation would be very expensive and even nonfeasible in many cases, only for the sake of research purposes the examined screening materials are assumed to be composed of the selected isotopes in 100% isotopic abundance. Nevertheless this isotopic study could be helpful in case that the enrichment of a selected element with respect to a particular isotope would be deemed as technoeconomically worthwhile. In all examined cases a thickness of 3 cm was considered.

As can be seen in Table 2 the densities of most isotopes are quite small; thus only ^{197}Au and ^{139}La could be of interest. In fact all isotopes below ^{139}La provided negligible spectrum modification, indicating that their macroscopic elastic scattering cross sections were inadequate to affect the spectrum

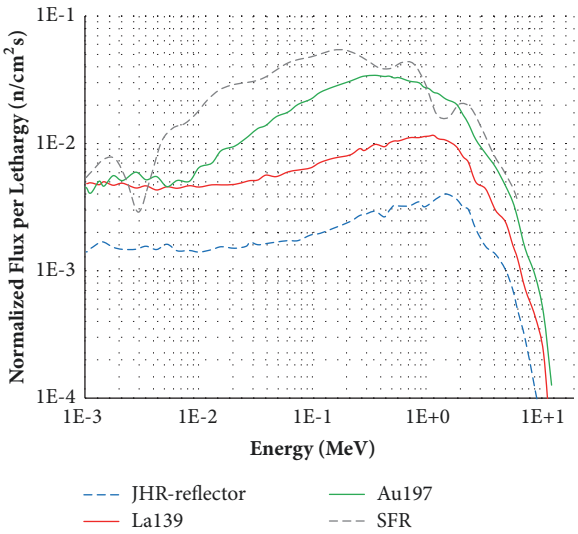

Figure 9: Effect of ^{139}La- and ^{197}Au-based screen on the JHR reflector neutron spectrum.

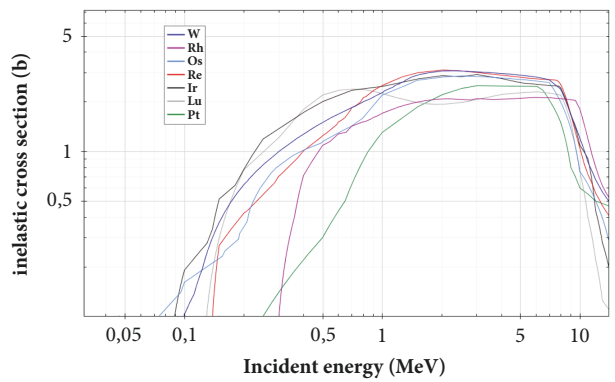

Figure 10: Inelastic microscopic cross sections of W, Rh, Os, Re, Ir, Lu, and Pt.

at high energies. Screens based on the heavier isotopes, i.e., ^{139}La and ^{197}Au, provided a neutron spectrum tailoring towards the desired direction (Figure 9). The more intense result of ^{197}Au is attributed not only to its density (higher than ^{139}La) but also to the combined effect of inelastic scattering (threshold at 0.1MeV).

5.3. Effect of Materials with Important Inelastic Scattering Capability. In this section the various materials efficiency to affect as desired the thermal neutron spectrum through inelastic scattering is investigated. The neutron energy boundaries of the JHR range between 1·10-11 and 20 MeV (thermal reactor) with the part from 1·10-9 to 10 MeV being of greater importance. Neutrons of higher energy almost always interact with nuclei by inelastic scattering. The reaction channel opens at a threshold energy recorded over 10 keV and mainly around 100 keV for heavy nuclei and a few MeV for light nuclei [58]. The maximum inelastic cross section is around 5 barns while for most nuclei it is around 1 barn [59]. Regarding the goal of the current investigation, the advantages of inelastic scattering in comparison to elastic are related to the substantial energy loss during collisions, as well as to the energy range where the reaction occurs, that is, in high energies. However, the low probability (i.e., small cross section) of inelastic reactions is a disadvantage that can be surpassed with the utilization of materials of high densities and/or in important quantities. Figure 10 highlights the low probability of inelastic neutron scattering for some representative materials (W, Rh, Os, Re, Ir, Lu, and Pt).

To study the inelastic scatterers' effect on the thermal neutron spectrum, a large set of numerical experiments with 57 different elements at their natural composition was carried out. A 3.4cm thick screen inserted in the irradiation facility was considered in each case. It is worth noting that, as in the case of elastic scatterers, a study with isotopes instead of natural elements might have been more indicative since different isotopes interact differently with neutrons; however such a study was here avoided as requiring a huge amount of calculations. Nevertheless after a successful result for a particular element an isotopic study can be carried out in order to investigate which isotopes mainly cause the spectrum tailoring. The number of tested elements was limited to 57 since in many cases the neutron cross section data were unavailable in JEFF-3.1 library. In addition, some elements such as minor actinides were excluded due to safety issues. Also elements with low densities (gases) and/or short half-lives were excluded.

In Figure 11, the 57 studied elements are presented. The elements of the first row presented maximum left-shifting and broadening of the spectrum in the high energy region while they provided substantial cutoff of the thermal component (Figure 12). The elements of the second row present a less sufficient shifting and broadening of the fast spectrum component, although they did provide a cutoff in the thermal area of the spectrum (Figures 13 and 14). Finally, the elements of the third row also presented maximum shifting and broadening of the fast spectrum component but negligible cutoff of the thermal component. Figure 15 presents the results for the third row elements (except for Si, which provided an almost identical spectrum to the JHR spectrum and thus, for clarity reasons, it was not included in the plot). The rest of the examined elements did not present any worth mentioning spectrum tailoring.

The results of Figure 11 are shown more representatively in Figure 16. The elements' efficiency in the neutron spectrum tailoring is represented with the same color coding used in Figure 11. As it can be seen W, Re, Os, Ir, and Pt are successive transition metals of the 6th period, while Rh (also transition metal) belongs to the immediately preceding period. Lu is lanthanide but belongs also to the 6th period. All elements belong to the d-block. Regarding density, Os and Ir are the denser elements, followed by Pt, Re, and W. Since these elements are sequential on the periodic table and with close density values their neutron number density will be similar as well. Furthermore Os, Re, W, and Ir have similar inelastic scattering cross sections (σ) with maximum (3 b) occurring

Re	W	Lu	Os	Rh	Pt	Ir
Pd	Tb	Ho	Ag	Cd	Ta	
Tl	Rb	As	Ru	Si		
Al	B	Bi	C	Ce	Co	Cr
Zr	Cs	Cu	Dy	Er	Eu	Fe
Ga	Gd	Ge	Hf	Hg	I	In
Mg	Mn	Mo	Nb	Nd	Ni	P
Pr	Sb	Sc	Se	Sn	Sr	Te
Ti	V	Y	Zn			

Figure 11: The elements whose effect on the thermal neutron spectrum due to inelastic scattering was examined.

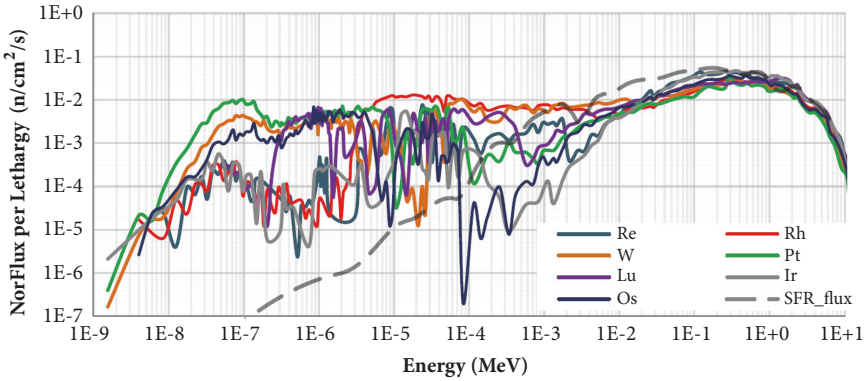

Figure 12: Effect of 3.4 cm Re, Rh, W, Pt, Lu, Ir, and Os neutron screens on the neutron spectrum. All screens provide a sufficient neutron spectrum shifting and broadening as well as thermal component cutoff.

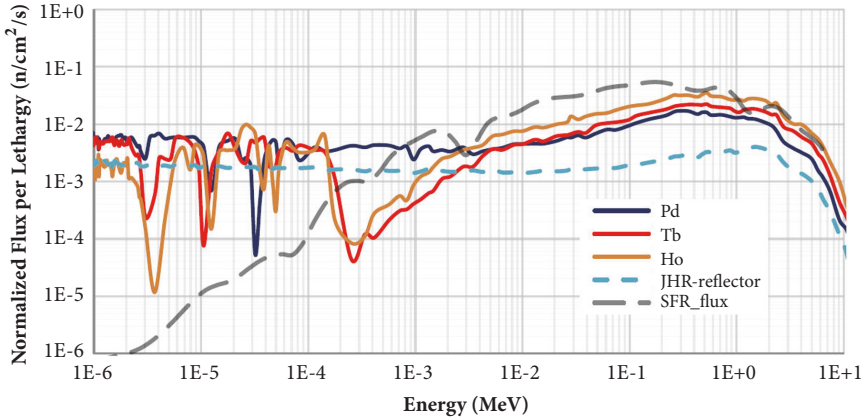

Figure 13: Effect of 3.4 cm Ho, Tb, and Pd neutron screens on the neutron spectrum. The neutron spectrum shifting and broadening are not sufficient. JHR reflector and SFR spectra are included for comparison.

between 1MeV and 5 MeV, while Pt, Lu, and Rh have lower σ with maximum occurring at ~2MeV.

The effect of the materials which better approach the desired spectrum modification in the high energies area (Figure 12) is better illustrated focusing on this specific part of the spectrum (Figure 17). The results indicate that a further broadening and extra shifting of the flux peak to lower energies would provide a neutron distribution more representative of SFR. This could be achieved by combining the above examined scatterers with other elements, the latter presenting enhanced inelastic scattering at lower energies. To investigate this possibility various tests were made for elements with notable inelastic cross section at lower energies, i.e., below ~1 MeV. Although with questionable feasibility (due to the low half-life of 72 days and to the requirement of isotope production) ^{160}Tb was tested exclusively for research purposes, this particular element was selected as presenting a characteristic inelastic cross section (Figure 18) with a peak at 1MeV. Combinations of Os and ^{160}Tb were tested with various ratios. For more representative results all the available space of 4.4 cm was utilized. Figure 19 shows the combined effect of the two elements in the thermal neutron spectrum. The result obtained by using only Os (0 ^{160}Tb:1Os) is also included for comparison. As can be seen a neutron screen composed of Os and ^{160}Tb in a 1:4 ratio modifies the neutron energy spectrum providing a quite satisfactory imitation of

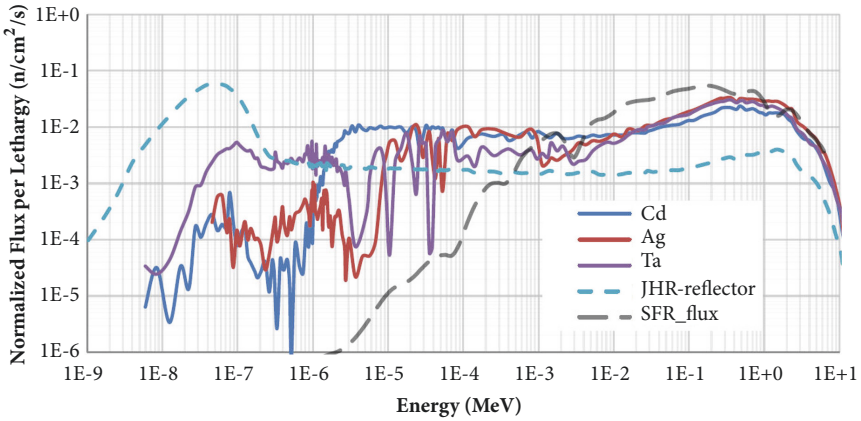

Figure 14: Effect of 3.4 cm Cd, Ag, and Ta neutron screens on the neutron spectrum. The neutron spectrum shifting and broadening are not sufficient. JHR reflector and SFR spectra are included for comparison.

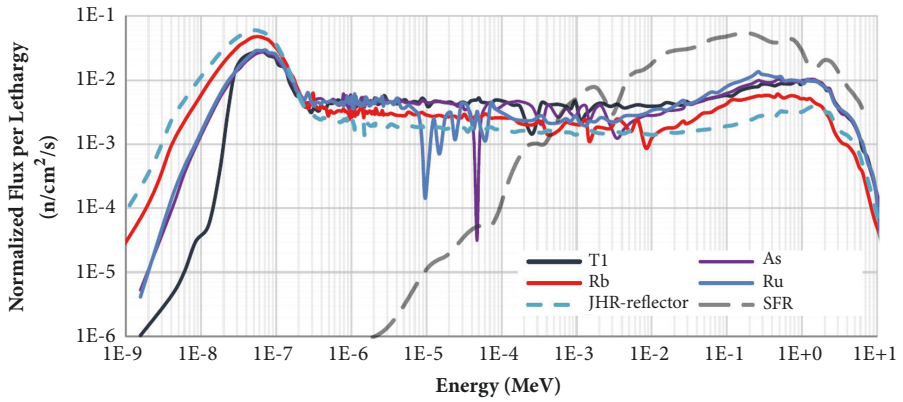

Figure 15: Effect of 3.4 cm Tl, As, Rb, and Ru neutron screens on the neutron spectrum. All screens provided sufficient neutron spectrum shifting and broadening but negligible thermal absorption capability.

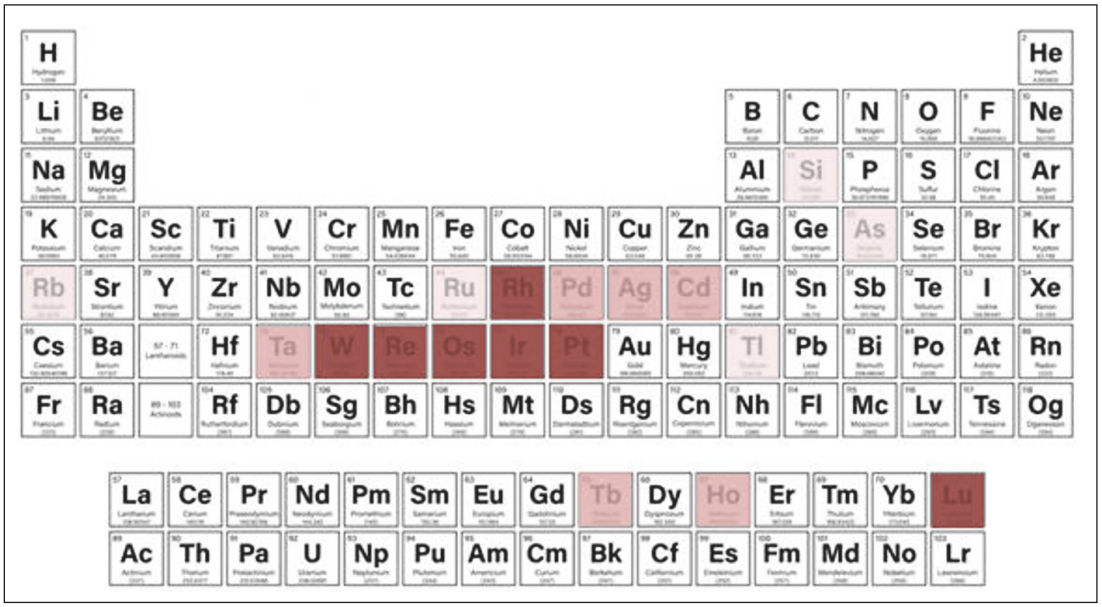

Figure 16: Effective inelastic scatterers labeled on the periodic table. Their relative efficiency in shifting and broadening the neutron flux peak in the JHR reflector towards lower energies and their ability to cut off the spectrum thermal component are indicated.

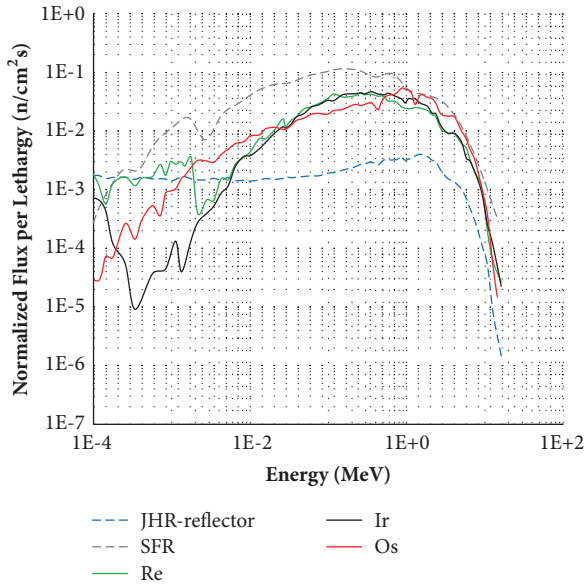

Figure 17: Effect of 3.4 cm thick neutron screens composed of Ir, Os, or Re on the JHR reflector neutron spectrum.

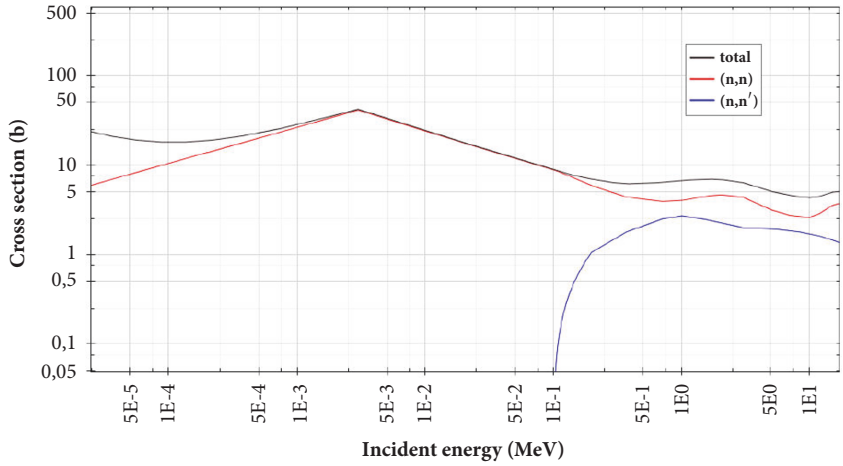

Figure 18: Total, elastic, and inelastic microscopic cross section of ^{160}Tb.

the SFR case. This result shows that proper combinations of screening materials can lead to the desired result, provided that mechanical fabrication is feasible.

Regarding the immediately less efficient scatterers (light red in Figure 16), the results for Ho are indicatively presented. ^{165}Ho is the only isotope of the solid holmium. Its neutron inelastic scattering channel opens at 0.1MeV with inelastic σ at about 1b; this increases with energy to reach finally 3b at 1MeV [38]. The small inelastic scattering cross section of ^{165}Ho imposed a large screen thickness, which at the same time caused a deeper flux depression at about 0.2keV, acting thus as a natural separator between high- and low-intermediate neutron energies; this created a clear part in the spectrum composed of high energy neutrons. It is worth noting that the depression of the neutron flux corresponds to the resonances of the capture and elastic cross sections. Figure 20 shows the results for varying screen thickness.

For further investigation of the effect of ^{165}Ho, fissile material (U, 20% enriched in U-235) of 1.0 cm was added in the conceptual screen, placed among the holmium and the irradiation space (Figure 21). As expected this combination enhanced the fast neutron spectrum component as well as the neutron flux within the irradiation space. The results are illustrated in Figure 22. It is noteworthy that the addition of booster enhances the fast spectrum component in such extent that fission neutrons are not adequately moderated by their scattering interactions with ^{165}Ho nuclei, as happens without fissile material. However, the combination of ^{165}Ho with fissile material results in higher neutron fluxes (by ~6 times), with a neutron distribution having reduced epithermal component.

5.4. Effect of Coolant. Since energy is deposited to the neutron screen device, the cooling of the screen is mandatory.

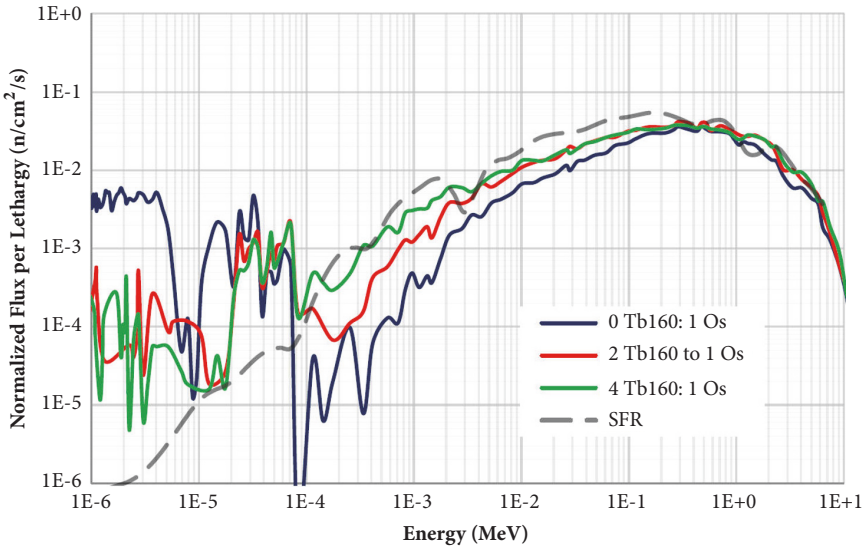

Figure 19: Effect on the neutron spectrum of a neutron screens with different Os and ^{160}Tb combinations.

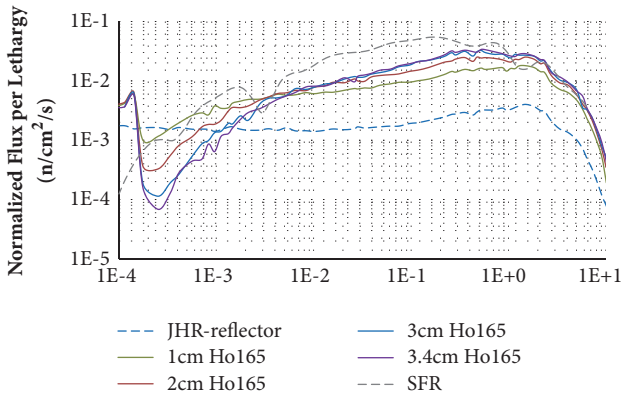

Figure 20: Effect of ^{165} Ho on the reference JHR spectrum for varying screen thickness.

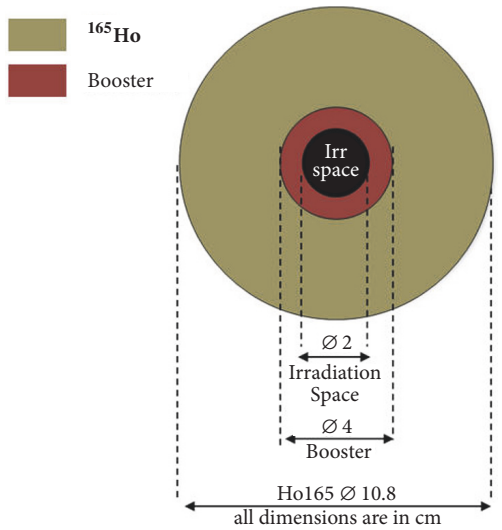

Figure 21: Irradiation device constituted by ^{165}Ho in combination with a booster (fissile material).

The materials used for cooling, however, might alter the performance of the neutron screen. To avoid this, cooling materials that are expected to induce minimum spectrum alterations were assumed in the present work, such as liquid helium and sodium. To confirm their minor effect on the neutron spectrum, relevant calculations were performed. In this respect a neutron screen totally composed of ^{4}He was considered for examining the material effect on the reference neutron spectrum; for ^{23}Na, 1cm booster fuel was also included and the spectra, with and without ^{23}Na, were compared to each other. The results are presented in Figures 23 and 24 for ^{4}He and ^{23}Na, respectively. As can be seen in Figure 23, the provided spectrum is almost identical to the reference one, except at the energy area around 1 MeV, where a weak tailoring can be observed. At 1 MeV, where the cross section of ^{4}He exhibits a peak, a flux depression occurs; neutrons with energies around 1 MeV experience a slight energy loss. In addition, a slight peak occurs at the left of the

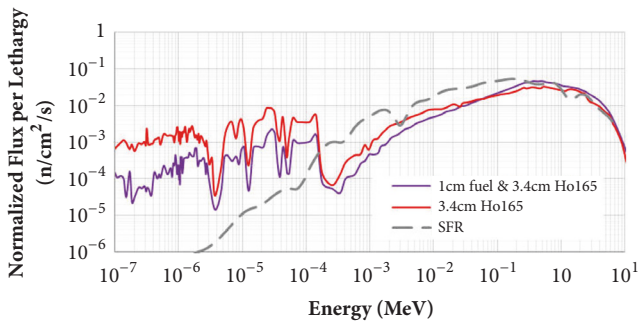

Figure 22: Effect on the neutron spectrum of 3.4 cm thick ^{165}Ho screen with and without 1cm fissile material.

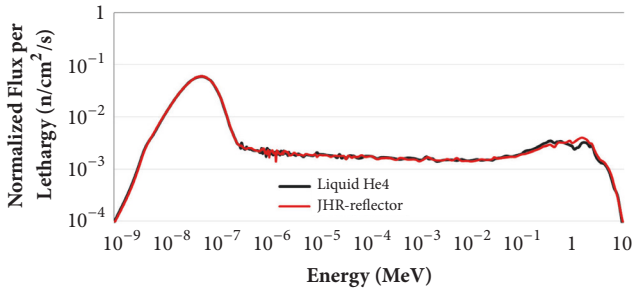

FIGURE 23: Effect of a 3 cm thick liquid ^{4}He layer on the neutron spectrum.

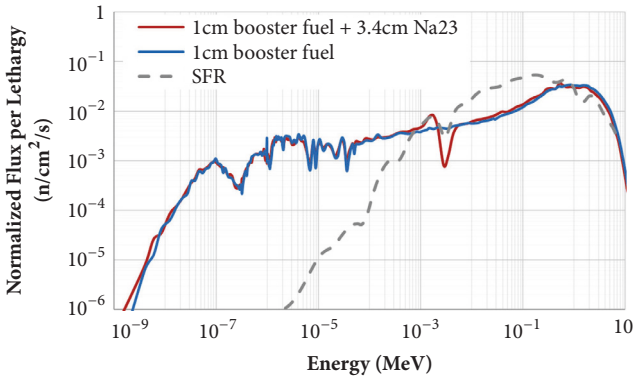

FIGURE 24: Effect of a 3.4 cm thick ^{23}Na layer on the neutron spectrum.

flux depression due to neutron moderation. As far as sodium coolant is concerned, it can be seen in Figure 24 that only a flux depression around 3 keV is provided corresponding to ^{23}Na elastic scattering resonance.

Based on the above findings, the various neutron screen materials were tested in this preliminary investigation without including the coolant effect; it should be noted however that the possible degradation of the neutron screen efficiency due to a selected coolant will require a more complete study.

6. Concluding Remarks

The goal of this study was to classify potential screening materials for locally transforming a thermal neutron spectrum to that of SFR. The neutron energies in a thermal reactor range between 1·10-11 and 20 MeV, with the part from 1·10-9 to 10 MeV being of greatest importance. The notable neutron interactions within this energy range include capture (radiative capture and fission) and scattering, elastic and inelastic.

The thermal neutron absorbers, even in screens of small thickness (e.g., 0.1 cm), can cause significant cutoff of the thermal neutrons' component in the neutron energy spectrum. Therefore they may be utilized for locally simulating a neutron spectrum of a fast reactor but not of SFR. The addition of fissile material (booster) amplifies the neutron spectrum component in high energies but essentially does not help for the SFR spectrum reproduction.

The inadequacy to simulate the SFR spectrum when based on neutron capture interactions (i.e., using absorbing and fissile screening materials) imposed the utilization of elements which present intense elastic and inelastic cross sections at the desired energy range (0.1-10MeV). The present work showed that the most critical parameters, which classify an element as effective inelastic scatterer, comprise the density, the inelastic microscopic cross section, and the energy range in which inelastic scattering occurs for this element. By using screening materials with high density and important inelastic scattering cross section in an energy range around 1 MeV the thermal neutron spectrum can be locally tailored so as to satisfactorily approach the typical distribution of the SFR spectrum.

Conceptual neutron screens composed of Os, Re, and Ir were found to provide a spectrum with neutron distribution similar to that of SFR, i.e., quite symmetrical around a maximum of 0.153MeV. However at energies E below 0.1MeV the tailored neutron spectrum did not exactly simulate that of SFR. An extra shifting of the flux peak to lower energies can give a more representative distribution, obtained by combining the above scatterers with materials for which inelastic scattering occurs at lower energies. This might be viewed provided that the required mechanical fabrication is feasible.

In the end it should be stressed that the introduction of a neutron screen device in a reactor's irradiation facility demands a comprehensive and exhaustive examination, the present work regarding only the first step, i.e., part of the study of the screening materials' effect on the neutron spectrum; more specifically the materials' physical (e.g., density) and neutronic (i.e., microscopic cross sections for the various reactions) properties are here considered. The subsequent investigation steps before the neutron screen implementation should comprise various topics regarding at least (a) the device impact on the reactor core reactivity and on the neighboring experiments, (b) the thermophysical properties of the screen, (c) the energy deposition, (d) the coolant medium, and (e) the device fabrication process and necessary postirradiation services. The present study focuses only on the first step of a complete investigation towards the target of achieving the desired neutron spectrum modification; that is, it deals with the neutronic behavior of each screening material. By examining a wide range of different screening materials, the present analysis can constitute the basis for all the subsequent material selection steps.

Abbreviations

ASTRID: Advanced Sodium Technological Reactor for Industrial Demonstration
ATR: Advanced Test Reactor
BR2: Belgian Reactor 2
BRR: Budapest Research Reactor
CFR-600: Cooled Fast Reactor-600
fnfm: Fast neutrons' flux maximum
FR: Fast reactor
Gen IV: Generation IV
GIF: Generation IV International Forum

HFIR: High Flux Isotope Reactor
HFR: High Flux Reactor
JHR: Jules Horowitz Reactor
JSFR: Japan Sodium cooled Fast Reactor
MITR: MIT Reactor
MTR: Material Testing Reactor
NPP: Nuclear Power Plant
PGSFR: Prototype Generation IV Sodium cooled Fast Reactor
PRISM: Power Reactor Innovative Small Module
SFR: Sodium fast reactor.

Data Availability

The data that support the findings of this study are openly available in NEA at http://www.oecd-nea.org/dbforms/data/eva/evatapes/jeff_31/index-JEFF3.1.1.html and http://www.oecd-nea.org/janis/.

Conflicts of Interest

The authors declare that they have no conflicts of interest.

Acknowledgments

This research paper has been cofinanced by the European Union (European Social Fund—ESF) and by the Greek national funds through the Operational Program "Education and Lifelong Learning" of the National Strategic Reference Framework (NSRF)—Research Funding Program: Thales. Investing in Knowledge Society through the European Social Fund.

References

[1] K. Aoto, P. Dufour, Y. Hongyi et al., "A summary of sodium-cooled fast reactor development," *Progress in Nuclear Energy*, vol. 77, pp. 247–265, 2014.

[2] OECD/NEA, "Generation IV International Forum, 46, quai Alphonse Le Gallo, 92100 Boulogne Billancourt (France) (2016). Generation 4 International Forum (GIF) 2015 Annual Report (NEAGIF-RA-2015)," Tech. Rep., OECD (Organisation for Economic Cooperation and Development) / Nuclear Energy Agency (NEA), 2016.

[3] J. E. Kelly, "Generation IV international forum: a decade of progress through international cooperation," *Progress in Nuclear Energy*, vol. 77, pp. 240–245, 2014.

[4] IAEA, "Fast Reactors and Related Fuel Cycles: Challenges and Opportunities (FR09) Proceedings of an international conference," Tech. Rep., IAEA (International Atomic Energy Agency), Division of Nuclear Power and Division of Nuclear Fuel Cycle and Waste Technology, Vienna, Austria, 2012.

[5] P. Yvon, M. Le Flem, C. Cabet, and J. L. Seran, *Structural Materials Challenges for Next Generation Nuclear Systems: Challenges and The Path Forward*, Bhabha Atomic Research Centre, India, 2014.

[6] OECD/NEA, "Le Seine Saint-Germain, 12 boulevard des Iles, F-92130 Issy-les-Moulineaux (France) (2011). Experimental facilities for sodium fast reactor safety studies - Task Group on Advanced Reactor Experimental Facilities (TAREF)," Tech. Rep., OECD (Organisation for Economic Cooperation and Development)/Nuclear Energy Agency (NEA), 2011.

[7] N. Chrysanthopoulou, P. Savva, M. Varvayanni, and N. Catsaros, "Compilation of existing neutron screen technology," *Science and Technology of Nuclear Installations*, vol. 2014, Article ID 395795, 23 pages, 2014.

[8] L. Vermeeren, P. Benoit, and J. Dekeyser, "uel power transient system developments – Design of in-core devices: Final report on the VANESSA-RODEO design," MTR+I3 Technical Report FI6O-656-036440, 2009.

[9] D. Moulin, L. Vermeeren, K. Bakker, C. Roth, and J. L. Rodriguez, "Fuel Testing Devices: Power Transient systems and neutron screen development for LWRs: Assessment of the type of transients to be achieved," MTR+I3 Technical Report FI6O-656-036440, 2007.

[10] S. Van Dyck, E. Koonen, M. Verwerft, M. WΘber, and M. Wéber, "Experimental Irradiations of Materials and Fuels in the BR2 Reactor: An Overview of Current Programmes (IAEA-TECDOC-1715)," Tech. Rep., International Atomic Energy Agency (IAEA), 2013.

[11] Ch. De Raedt, E. Malambu, B. Verboomen, and Th. Aoust, "Increasing complexity in the modeling of BR2 irradiations," in *Proceedings of the PHYSOR 2000 International Topical Meeting on Advances in Reactor Physics and Mathematics and Computation into the Next Millennium*, Pittsburg, Calif, USA, 2000.

[12] C. Reynard, J. Andre, J. Brun et al., "In core instrumentation for online nuclear heating measurements of material testing reactor (INIS-BE–10K0001)," Tech. Rep., Belgium, 2010.

[13] A. Zeman, K. Tuček, L. Debarberis, and A. Hogenbirk, "High intensity positron source at HFR: Basic concept, scoring and design optimisation," *Nuclear Instruments and Methods in Physics Research Section B: Beam Interactions with Materials and Atoms*, vol. 271, pp. 19–26, 2012.

[14] G. Eynde, J. Dekeyser, L. Vermeeren et al., "Neutron screen technology: Overview neutron screen technology," MTR+I3 Technical Report FI6O-656-036440, 2009.

[15] G. Eynde, J. Dekeyser, L. Vermeeren et al., "Neutron screen technology: Simulation of fast neutron spectrum in MTR," MTR+I3 Technical Report FI6O-656-036440, 2009.

[16] J. McDuffee, J. C. Gehin, R. J. Ellis, R. W. Hobbs, T. Primm, and T. Primm III, "Proposed fuel pin irradiation facilities for the high flux isotope reactor (ORNL/PTS-9878)," Tech. Rep., American Nuclear Society, 2008.

[17] N. Xoubi, R. T. Primm, and R. T. Primm III, "Modeling of the High Flux Isotope Reactor Cycle 400 (ORNL/TM-2004/251)," Tech. Rep., Oak Ridge National Laboratory, Oak Ridge, Tenn, USA, 2004.

[18] J. C. Gehin, R. J. Ellis, and J. McDuffe, "Development of fast spectrum irradiation facility for fuels development in the high flux isotope reactor," in *Proceedings of the ARWIF 2008 - Workshop on Advanced Reactors with Innovative Fuels*, Fukui, Japan, 2008.

[19] D. P. Guillen, L. Porter, L. Douglas, J. R. Parry, and H. Ban, "In-pile experiment of a new hafnium aluminide composite material to enable fast neutron testing in the advanced test reactor (INL/CON-10-17879)," in *Proceedings of the ICAPP '10*, San Diego, Calif, USA, 2010.

[20] G. R. Longhurst, D. Guillen, J. R. Parry, D. L. Porter, and B. W. Wallace, "Boosted fast flux loop alternative cooling assessment (INL/EXT-07-12994)," Tech. Rep., Idaho National Laboratory, 2007.

[21] F. Marshall, "Advanced test reactor capabilities and future operating plans (INL/CON–05-00549)," Tech. Rep., Idaho National Laboratory, 2005.

[22] G. S. Chang and R. G. Ambrosek, "Hardening neutron spectrum for advanced actinide transmutation experiments in the ATR," *Radiation Protection Dosimetry*, vol. 115, no. 1–4, pp. 63–68, 2005.

[23] K. Sun, *Analysis of advanced sodium-cooled fast reactor core designs with improved safety characteristics [Ph.D. thesis]*, EPFL, 2012, http://infoscience.epfl.ch/record/181222.

[24] T. Ellis and T. Newton, "Innovations in design for the enhancement of experimental neutron flux at the Massachusetts Institute of Technology research reactor," in *Proceedings of the International Congress on Advances in Nuclear Power Plants*, Anaheim, Calif, USA, 2008.

[25] T. S. Ellis, *Design of a low enrichment, enhanced fast flux core for the MIT research reactor [Ph.D. thesis]*, Massachusetts Institute of Technology, 2009.

[26] R. J. Ellis, "Comparison of calculated and measured neutron fluence in fuel/cladding irradiation experiments in HFIR," *Transactions of the American Nuclear Society*, vol. 105, pp. 808–810, 2011.

[27] F. W. Ingram, A. J. Palmer, and D. J. Stites, "Temperature controlled material irradiation in the advanced test reactor," *Journal of Nuclear Materials*, vol. 258-263, pp. 362–366, 1998.

[28] G. S. Chang, R. G. Ambrosek, and F. W. Ingram, "ATR Al-B neutron filter design for fusion material experiment," *Fusion Engineering and Design*, vol. 63-64, pp. 481–485, 2002.

[29] A. Horvath and A. Brolly, "Neutron screen technology: Report evaluation of new types of absorbers," MTR+I3 Technical Report FI6O-656-036440, 2009.

[30] B. Pond, A. Hanan, J. E. Matos, and C. Maraczy, "Neutronic safety parameters and transient analyses for potential LEU conversion of the Budapest Research Reactor (INIS-XA-C–003," 1999.

[31] C. Vitanza, "Overview of the OECD-Halden reactor project," *Nuclear Engineering and Design*, vol. 207, no. 2, pp. 207–221, 2001.

[32] B. Volkov, M. McGrath, and T. Tverberg, "In-pile experimental investigations of fuels and materials degradation in the Halden reactor," in *Proceedings of the 11th International Conference on WWER Fuel Performance, Modelling And Experimental Support Proceedings*, M. Mitev, Ed., p. 712, Institute for Nuclear Research and Nuclear Energy, Bulgaria, 2015.

[33] IAEA, "Fuel behaviour and modelling under severe transient and loss of coolant accident (LOCA) conditions proceedings of a technical meeting (IAEA-TECDOC-CD–1709)," Tech. Rep., International Atomic Energy Agency, Nuclear Fuel Cycle and Material Section, Vienna, Austria, 2003.

[34] B. Duc, B. Biard, P. Debias, L. Pantera, JP. Hudelot, and F. Rodiac, "Renovation improvement and experimental validation of the Helium-3 transient rods system for the reactivity injection in the CABRI reactor," in *Proceedings of the IGORR 2014 conference*, Bariloche, Argentina, 2014.

[35] J. P. Hudelot, Y. Garnier, J. Lecerf, M. Fournier, S. Magnetto, and E. Gohier, "CABRI reactor commissioning: results and analysis of the tests on the primary cooling system and on the control and safety rods," in *Proceedings of the IGORR 2014 conference*, Bariloche, Argentina, 2014.

[36] J. P. Hudelot, "CABRI facility: upgrade, refurbishment, recommissioning and experimental capacities," in *Proceedings of the PHYSOR 2016*, Sun Valley, Idaho, USA, 2016.

[37] D. Imholte and F. Aydogan, "Comparison of nuclear pulse reactor facilities with reactivity-initiated-accident testing capability," *Progress in Nuclear Energy*, vol. 91, pp. 310–324, 2016.

[38] JEFF-3.1.1, 2016, http://www.oecd-nea.org/dbforms/data/eva/evatapes/jeff_31/index-JEFF3.1.1.html.

[39] JANIS 4, 2018, http://www.oecd-nea.org/janis/.

[40] G. Bignan, C. Colin, J. Pierre et al., "The Jules Horowitz Reactor research project: a new high performance material testing reactor working as an international user facility-first developments to address R&D on material," *The European Physical Journal Conferences*, vol. 115, Article ID 01003, 2016.

[41] G. Bignan, X. Bravo, and P. M. Lemoine, "The Jules Horowitz Reactor, a new high performances European MTR (material testing reactor) with modern experimental capacities toward an international centre of excellence," in *Proceedings of the International Group on Research Reactors (RRFM 2012)*, Prague, Czech Republic, March 2012.

[42] C. P. Console, *Power transient analysis of experimental devices for Jules Horowitz material testing reactor (JHR) [Ph.D. thesis]*, University of Bologna, 2013, http://amsdottorato.unibo.it/5689/.

[43] D. Parrat, G. Bignan, B. Maugard, C. Gonnier, and C. Blandin, "The future Jules Horowitz material testing reactor: An opportunity for developing international collaborations on a major European irradiation infrastructure," in *Proceedings of the 11th International Conference on WWER Fuel Performance, Modelling and Experimental Support Proceedings*, M. Mitev, Ed., Bulgaria, 2015.

[44] O. Petit and F. X. Hugot, "RIPOLI-4 Version 8 User Guide (SERMA/LTSD/RT/11-5185/A)," Tech. Rep., 2001.

[45] W. S. Yang, "Fast reactor physics & computational methods," *Nuclear Energy Technology*, vol. 44, no. 2, pp. 177-178, 2012.

[46] J. B. Nims and P. F. Zweifel, "Preliminary report on sodium temperature coefficients in large fast reactors (APDA-135)," Tech. Rep., 1959, http://www.osti.gov/scitech/servlets/purl/4170712.

[47] J. Guidez, D. Goux, and R. Dupraz, *Phenix, A Unique Research Reactor in Europe. Research Means to Back The Development of Nuclear Reactors*, 2005.

[48] IAEA, "Phenix and Super-Phenix reactors (IAEA-TECDOC-1569)," Tech. Rep., International Atomic Energy Agency, Nuclear Power and Technology Development Section, 2007.

[49] A. Chenu, R. Adams, K. Mikityuk, and R. Chawla, "Analysis of selected Phenix EOL tests with the FAST code system Part I: Control-rod-shift experiments," *Annals of Nuclear Energy*, vol. 49, pp. 182–190, 2012.

[50] D. W. Muir, "NJOY: a comprehensive system for the processing of endf formatted nuclear data," in *Reactor Physics Calculations for Applications in Nuclear Technology*, pp. 55–62, 1991.

[51] E. Brun, F. Damian, C. M. Diop et al., "Tripoli-4®, CEA, EDF and AREVA reference Monte Carlo code," *Annals of Nuclear Energy*, vol. 82, pp. 151–160, 2015.

[52] NEA, "NEA-1716 TRIPOLI-4 VERS. 8.1," Tech. Rep., 2013.

[53] R. Sanchez, J. Mondot, Z. Stankovski, A. Cossic, and I. Zmijarevic, "APOLLO II: A user-oriented, portable, modular code for multigroup transport assembly calculations," *Nuclear Science and Engineering*, vol. 100, no. 3, pp. 352–362, 1988.

[54] R. Jacqmin, J. Tommasi, D. Bernard, and A. Santamarina, "Improved reactor core calculations with JEFF-31 data," in *Proceedings of the International Conference on the Physics of Reactors "Nuclear Power: A Sustainable Resource"*, Interlaken, Switzerland, 2008.

[55] N. Chrysanthopoulou, G.-K. Delipei, P. Savva, M. Varvayanni, and N. Catsaros, "Computational study of neutron screens performance considering different absorbing materials," in *Proceedings of the NENE 2014 International Conference Nuclear Energy for New Europe*, Portoroz, Slovenia, 2014.

[56] N. Chrysanthopoulou, *Upgrade of the research and operational capabilities of nuclear research reactors [Ph.D. thesis]*, National Technical University of Athens, 2018.

[57] S. F. Mughabghab and D. I. Garber, *Neutron Cross Sections*, vol. I, Brookhaven National Laboratory, New York, NY, USA, 3rd edition, 1973.

[58] K. S. Krane, *Introductory Nuclear Physics*, Wiley & Sons, New Jersey, NJ, USA, 3rd edition, 1987.

[59] M. Litz, C. Waits, and J. Mullins, "Neutron-activated gamma-emission: technology review (ARL-TR-5871)," Tech. Rep., Adelphi: Army Research Laboratory, 2012.